

## Subpicosecond luminescence study of tunneling and relaxation in coupled quantum wells

B. Deveaud, A. Chomette, F. Clerot, P. Auvray, and A. Regreny  
*Centre National d'Etudes des Télécommunications (LAB/OCM), 22301 Lannion, France*

R. Ferreira and G. Bastard  
*Groupe de Physique des Solides de l'Ecole Normale Supérieure, 24 rue Lhomond, 75005 Paris, France*  
 (Received 12 April 1990)

We study, by time-resolved luminescence with subpicosecond resolution, the tunneling of electrons out of a narrow well (NW) coupled to a wider well (WW) by a thin barrier. The relative energy positions of the NW ground state and of the WW first excited level are changed by adjusting the WW width. Near resonance, and for narrow enough barriers, the transfer time of the electrons to the WW ground state is close to 2 ps and is analogous to LO-phonon-assisted intersubband relaxation. When the barrier thickness increases above 40 Å, this transfer time increases exponentially with the barrier thickness. The barrier thickness above which the variation becomes exponential strongly depends on the energy mismatch of the levels in the isolated wells and is indicative of interface roughness. The dependence of the decay times on barrier thickness for purposely misaligned samples is always exponential.

### I. INTRODUCTION

Tunneling is a physical phenomenon of interest from a device point of view as well as from more basic aspects. Two simple cases can be considered and studied thanks to the capabilities of modern growth techniques: the system of double-barrier resonant structures or the system of quantum wells coupled by a thin barrier. In terms of physics, the interest of these two systems lies in the fact that it is possible to grow and to study semiconductor structures that are purely quantum systems, and where the influence of scattering mechanisms can be reduced quite largely. Double-barrier resonant tunnel structures have been extensively studied for their possible high-frequency applications.<sup>1</sup> Different aspects have been considered such as switching time constant,<sup>2</sup> accumulation of carriers in the quantum well,<sup>3,4</sup> and escape time of electrons from the quantum well.<sup>5,6</sup> The possible coherence of the electron during the tunneling process has also been actively considered.<sup>7</sup>

Coupled quantum wells (CQW's) consist in two quantum wells separated by a thin barrier. The pattern may be repeated in the sample, each unit of CQW's being separated from the next one by a large barrier.<sup>8</sup> CQW's have attracted much interest recently.<sup>9-17</sup> One possible application would be the reduction of the recovery time constant after bleaching of the excitons in one quantum well, when coupled to another one through a thin barrier.<sup>8,18</sup> Other possible applications have recently been considered.<sup>19-21</sup> Of interest also are the possible tunneling mechanisms from one well to the other: various possible effects may lead to tunneling, either "on" or "off" resonance,<sup>22,23</sup> but the exact resonance between a level in the narrow well (NW) and a level in the wide well (WW) is expected to lead to the fastest mechanism.<sup>23</sup>

Tuning of the resonance between the ground state of the NW and the  $n = 2$  level of the WW has been obtained

by applying an electric field to a set of CQW's inside a pin junction.<sup>12,13,15,24</sup> Changes in the tunneling characteristics can be evidenced by a change in the intensity ratio between the NW and the WW lines in cw luminescence experiments,<sup>10</sup> or by a change in the time decay of the NW luminescence as a function of the applied field: a reduction from 70 ps in the "off-resonance" case down to 7 ps in the "on-resonance" case has been observed for CQW's with 50-Å barriers.<sup>15</sup> Some difficulties arise, however, in such experiments both due to the possible tunneling of holes<sup>12</sup> and to the effect of the injected carrier density on the actual field.<sup>12,13,15</sup>

We have studied a set of GaAs/Al<sub>x</sub>Ga<sub>1-x</sub>As CQW's by luminescence with subpicosecond resolution; the main information is the decay time of the luminescence corresponding to the NW (or to the levels in resonance). Both "on-resonance" and "off-resonance" samples are grown and studied as a function of the tunnel barrier thickness; we do not apply an electric field to the system. CQW's of a given barrier thickness (40 Å) are also studied and tuned on and off resonance by changing the WW thickness. Experimental decay times are then compared with computed relaxation times involving different mechanisms, the fastest one being Fröhlich interaction with optical phonons. A short account of the results published here was already published in Ref. 25.

### II. SAMPLES AND EXPERIMENTAL SETUP

GaAs/Al<sub>x</sub>Ga<sub>1-x</sub>As samples were grown by molecular beam epitaxy (MBE) and each consists of 25 periods of CQW's separated by a 150-Å barrier. Al content of the barriers is close to 26 at. %. Precise determination of the sample parameters (Al concentration in the barriers, thickness of the different layers) is obtained by x-ray diffraction and with the help of a model computation taking into account the whole structure of the sample. The

wells are selectively doped  $p$  type to a level of about  $10^{11}$   $\text{cm}^{-2}$ , the barriers are undoped. In the first series, designed to be “on resonance,” the well widths are kept at 60 and 140 Å, the barrier being changed from 75 to 30 Å (the well widths of 60 and 140 Å correspond approximately to the resonant case when taking into account the  $p$ -type doping and thus the transfer of roughly half of the holes from the NW to the WW). In the second series, designed to be “off resonance,” the well widths are kept to 60 and 120 Å, the barrier being changed from 80 to 15 Å [for this series, the samples are undoped: this increases the decay times by about a factor of 2 (Ref. 26)]. In the third series, the barrier is kept at about 40 Å, the NW at 60 Å, and the WW width is changed from 120 to 190 Å, thus changing the resonance conditions. In the following, the samples will be labeled according to the NW width, barrier width, and WW width in Å.

$p$ -type doping has been used for three reasons.

(i) Speeding up the cooling of electrons: the injected carrier density being at most 10% of the doping level, a fast cooling of the electrons is observed. It results in a much faster rise time of the luminescence curves,<sup>27</sup> as a matter of fact, the carrier temperature reaches about 80 K within less than 10 ps.

(ii) Selecting electron effects: any movement of the photocreated holes will have a negligible effect on the luminescence characteristics as long as the density is kept small compared to the doping level.

(iii) Improving the signal by the increase of the radiative recombination rate that is directly proportional to the doping level in the range of densities that we are using.<sup>28</sup>

One of the problems that we have to deal with is the possible buildup of a dipole at the interface due to the faster tunneling of electrons as compared to the holes. In all our experiments, we have checked whether we were working in a region of low enough densities: in such a case, the time constants that we observe do not change on lowering the excitation density.

Subpicosecond pulses are obtained by synchronous pumping of a double jet dye laser (model 702 Coherent Inc.), with the frequency doubled output of a yttrium aluminum garnet (YAG) laser (Antares, Coherent Inc.). We used 600-fs pulses with an average power of about 500 mW. Luminescence spectra are recorded with a resolution equivalent to the pulse width by mixing the luminescence photons with a delayed pulse of the laser.<sup>29,30</sup> The excitation energy is 2.04 eV, i.e., above the barriers, which creates a homogeneous excitation of the two wells at the shortest times. The short capture time<sup>31</sup> as well as the  $p$ -type doping ensure a rapid thermalization in each well: a short rise time of the WW luminescence, of the order of 20 ps (instead of about 200 ps in the case of undoped samples), at a lattice temperature of 20 K demonstrates this. Excitation densities can be adjusted from 0.2 up to 200 mW, with a spot diameter of 30  $\mu\text{m}$ , giving a photoexcited carrier density between  $10^{10}$  and  $10^{13}$   $\text{cm}^{-2}$  carriers per well.

### III. EXPERIMENTAL RESULTS

We shall first describe the technique used to obtain the parameters of our samples, then give the results obtained

in time-resolved luminescence with a low excitation density (about  $5 \times 10^{10}$   $\text{cm}^{-2}$  per well) and in a last part vary the excitation density in order to evidence possible saturation effects.

#### A. X-ray characterization of the CQW's

A correct interpretation of our results requires a precise knowledge of the parameters of the samples that have been realized: the ratio of the well widths is of particular importance. We have used x-ray-diffraction properties of the CQW structure in order to estimate the different parameters. These parameters are summarized in Fig. 1, they are the following: the NW width  $L_N$ , the barrier thickness  $L_b$ , the WW width  $L_W$ , the isolation barrier width  $L_i$ , the period  $C$  of the structure, and the composition  $x$  of the alloy barriers.

In a recent article,<sup>32</sup> Auvray *et al.* have shown that it was possible to assume a constant growth rate for each of the constituents (GaAs or  $\text{Al}_{1-x}\text{Ga}_x\text{As}$  layers) of a superstructure during the run. This reduces the number of unknown parameters of our structure to three only: the alloy composition  $x$ , the  $\text{Al}_{1-x}\text{Ga}_x\text{As}$  growth rate  $K_x$ ; then  $L_i = K_x t_i$  and  $L_b = K_x t_b$ , and the GaAs growth rate  $K_0$ ; then  $L_N = K_0 t_n$  and  $L_w = K_0 t_w$ , with obvious meaning for the different times  $t_j$ . With these assumptions the determination of the parameters of the CQW follows the usual procedure.

(a) The intensities and positions of the different high-order satellite peaks of the diffraction pattern are recorded with a  $\theta$ - $2\theta$  goniometer in the vicinity of the 002 Bragg reflection of the substrate.

(b) The average peak (zeroth-order satellite peak) is precisely recorded using the rocking curve technique in the vicinity of the 004 diffraction peak of the substrate. This allows to get the mean composition  $\bar{x}$  of the CQW structure. The mean composition  $\bar{x}$  can be obtained straightforwardly from our assumptions, and we get a very simple relation with once again three parameters only ( $x$ ,  $L_b$ , and  $C$ ):

$$\bar{x} = xL_b(1 + t_i/t_b)/C.$$

(c) The experimental profile is then compared with a

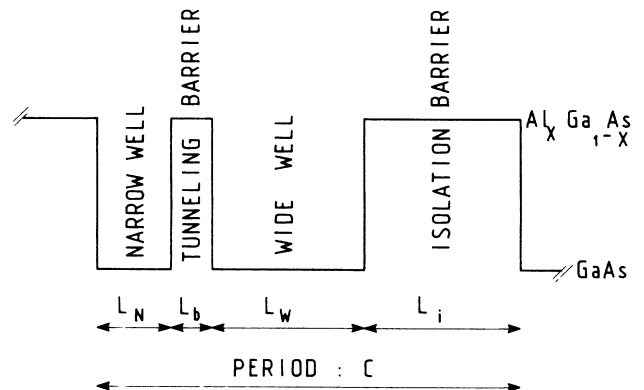


FIG. 1. CQW sample structure with important parameters.

computed diagram obtained from a kinematical model<sup>33</sup> that allows us to introduce noninteger values of the thickness in terms of atomic layers.

In Fig. 2 is shown the experimental diffraction diagram of one of the samples (No. 1), obtained in  $\theta$ - $2\theta$  configuration. The expected parameters are 60/40/120 with  $L_i = 150 \text{ \AA}$  and  $x = 0.26$ . The width of the different superlattice peaks as well as their large number are a direct indication of the high regularity of the structure, and of the absence of crystalline defects. The fitting procedure leads to the simulated diagram shown in Fig. 2 with values quite different from the expected ones. The sample is 77/47/154 with  $L_i = 180 \text{ \AA}$  and  $x = 0.25$ . The agreement between the calculated diagram and the experimental one is quite good. In particular, this set of values explains the systematic vanishing of the peaks for orders multiple of 6.

For the peaks of highest order, the agreement is not as good. Baudet *et al.*<sup>34</sup> have shown that the systematic difference, for the high-order peaks ( $i > 5$ ), between the experimental and the calculated diagrams was mainly due to the lateral composition gradient of our structures. We do not use a rotating substrate, and thus the composition is not constraint over the spot sampled by the x rays: typical variations of the growth rate would be of the or-

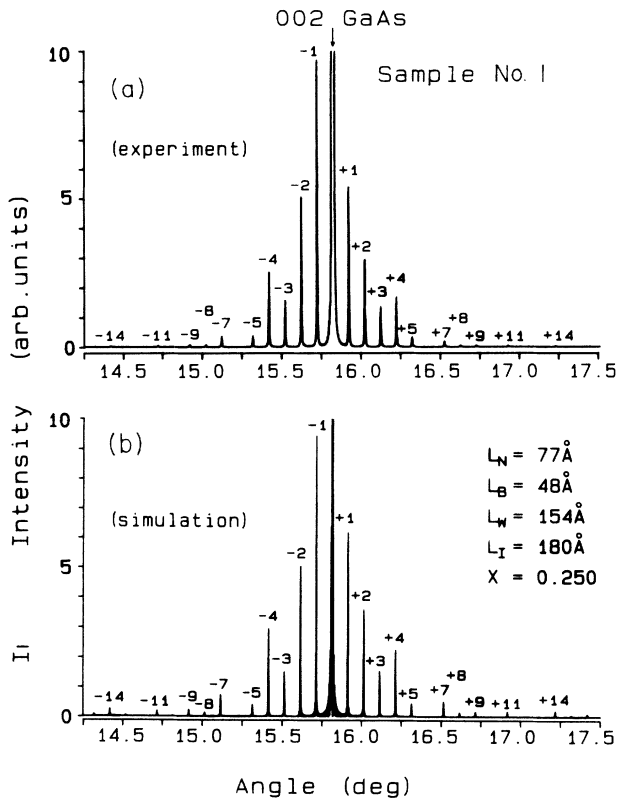


FIG. 2. (a) Experimental diffraction pattern of sample No. 1 obtained from  $\theta/2\theta$  configuration. The expected parameters of the sample are 60/40/120,  $L_i = 150 \text{ \AA}$ , and  $x = 0.3$ . (b) Calculated diagram with the following parameters: 77/48/154;  $L_i = 180 \text{ \AA}$ ,  $x = 0.25$ . Note that the growth rate was 15% larger than expected.

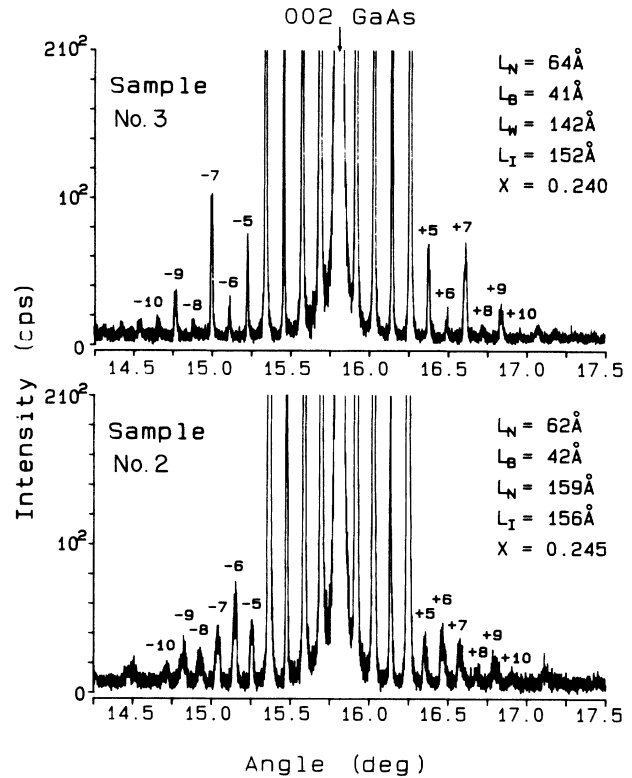


FIG. 3. Comparison between experimental spectra of two samples only differing by the WW thickness. The thickness variation is only 11% of  $L_w$  and leads to an easily observable change of the  $\pm 5$ ,  $\pm 6$ , and  $\pm 7$  satellites intensity. The parameters deduced from the fit are: for sample No. 2, 62/42/159, with  $L_i = 152$ ,  $x = 0.24$ ; for sample No. 3, 64/42/142, with  $L_i = 156$ ,  $x = 0.245$ .

der of 2% to 3% per cm.<sup>35</sup> This leads to a weaker intensity of the experimental peaks compared to the calculated ones.

In order to show the ability of x-ray diffraction to evidence small structural changes, we compare in Fig. 3 the experimental spectra of two samples, with very close parameters. The fitted parameters of the two samples are reported in Table I: this example demonstrates that, although the differences between the two samples are rather small, they can be deduced from the fit of the intensities of the high-order diffraction peaks.

In these two samples, the only significant difference is the width of the wide well: it changes from 142 to 159  $\text{\AA}$ , i.e., a relative difference  $\delta L_w / C$  of 4% only. This small change gives rise, both experimentally and theoretically, to a strong variation of the ratio of the intensities of the

TABLE I. Parameters of the two samples of Fig. 3, as deduced from the fitting procedure. Note that the main variation is the change of the WW thickness  $L_w$ .

	$L_n$	$L_b$	$L_w$	$L_i$	$x$
2	61.5	41.7	159	418.2	0.245
3	64	41	142	399	0.240

satellite peaks  $\pm 5$ ,  $\pm 6$ , and  $\pm 7$ .

These examples demonstrate the high sensitivity of x-ray diffraction to the internal structure of CQW's. The large number of satellite peaks has allowed us to determine, with sufficient precision, the parameters of our CQW samples. These parameters are the ones we used in the following of this paper, however, when we want to label a series of samples, we shall label them by their expected thicknesses, for example  $60/L_b/140$ .

### B. Low-density luminescence results

A typical set of luminescence spectra is shown in Fig. 4 for sample 64/41/142 (designed to "on resonance"). The spectrum at 2 ps delay after the excitation pulse shows two well-defined peaks, respectively, corresponding to the ground state  $n=1$  level of the WW (1.51 eV) and the first excited state composed of the coupled  $n=1$  level of the NW and the  $n=2$  level of the WW (1.57 eV). Note that all spectra are plotted on logarithmic scale. As a result of the band-gap renormalization<sup>36</sup> induced by the  $p$ -type doping of the samples, we observe a red shift of the luminescence peaks when compared to undoped samples. The high-energy slope of the two luminescence peaks corresponds to a mean carrier temperature of 205 K. After 10 ps only, the 1.57-eV line has almost vanished: all electrons are in the WW ground state. The effective temperature is now 60 K, showing the quite efficient thermalization of the photo-created electrons due to their interaction with the background holes. The temperature for 205 K at short times indicates the holes have been heated by the electrons, at least up to a temperature of 35 K. This observation is consistent with the fast cooling of the minori-

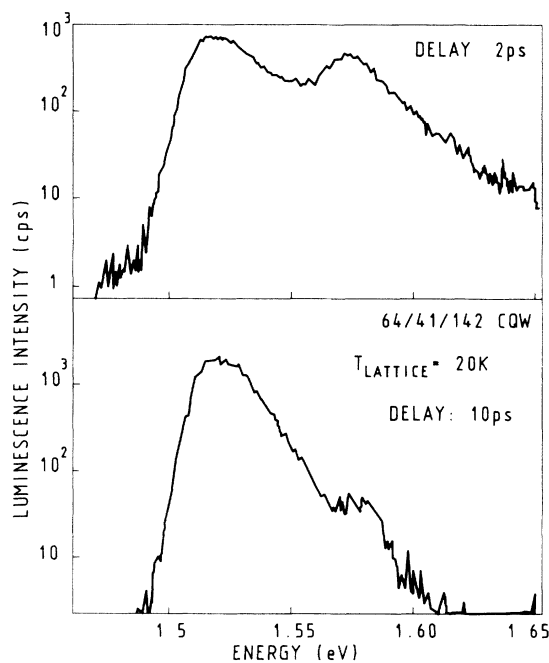


FIG. 4. Photoluminescence spectra of a 64/42/142 CQW system at two different delays (2 and 10 ps) after the excitation pulse. The sample is designed to be "on resonance." Intensity is in  $\log_{10}$  scale.

ty electrons observed here. If we assume that the holes have cooled back to lattice temperature (20 K) after 10 ps, then the electrons would be at about 87 K. More likely, electrons and holes will be at the same temperature after only a few picoseconds, and will cool down together.<sup>37</sup>

The 1.57-eV peak is weaker than the 1.51-eV one, although a homogeneous excitation of the two wells is expected to give a 1.57-eV luminescence at short times at least as intense as the 1.51-eV peak. This smaller intensity (observed in the different "on-resonance" samples with barrier thickness thinner than 40 Å) at the shortest times already indicates that a strong tunneling occurs during the first stages of capture and relaxation of the electrons in the wells. This is not unexpected as high-energy electrons will experience a very small barrier height.

For comparison, we show in Fig. 5 the equivalent behavior of the 62/43/195 sample. The characteristic time for the disappearance of the 1.55-eV luminescence is now much longer as a result of the tuning off of the resonance

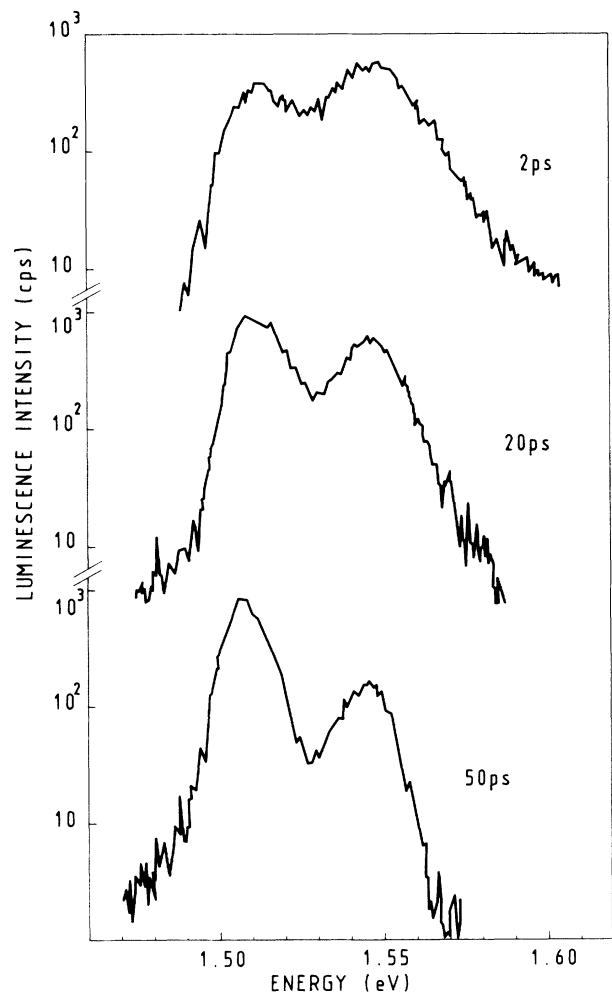


FIG. 5. Photoluminescence spectra of a CQW sample designed to be off resonance (63/41/194), at three different delays: 2, 20, and 50 ps. Intensity is in  $\log_{10}$  scale.

conditions. As tunneling is much slower in such a case, luminescence from the WW ground state at short times is indeed of the order of the luminescence coming from the NW.

The time behavior of the 1.57-eV luminescence peak intensity is plotted in Fig. 6 for the case of the 64/41/142 sample. The decay behavior is exponential over 1.5 orders of magnitude with a time constant of 2.2 ps. Although the decay times vary largely, the same kind of exponential decay is observed for all samples, designed to be "on" or "off" resonance, and for the different barrier thickness. In the case of long decay times, in extracting the tunneling times from the experimental values care has to be taken of the influence of radiative recombination in the observed decay time.<sup>16</sup> For the longest time, the data have to be taken at higher temperatures in order to increase the radiative lifetime.<sup>38</sup>

We have plotted in Fig. 7 the decay times observed on both series of samples as a function of the barrier thickness. Note the strong variation of the decay times when the barrier goes from 75 to 40 Å for the "on-resonance" samples and the saturation below 40 Å with times of the order of 2 ps. The error bars in the case of the samples with the thinnest barriers come from the very low intensity of the NW luminescence in these samples. The high-energy thermal tail from the WW cannot be neglected any more and a subtraction procedure has to be used leading to these error bars. For the series of "off-resonance" samples (60/ $L_b$ /120 with  $L_b = 15, 30, 40, 60,$  and 80 Å: this series is undoped), the dependence of the times on barrier thickness is exponential, the times being longer than in the "on-resonance" case by a factor of about 15. In both series, the energy separation between the two luminescence lines is larger than one LO-phonon energy.

In Fig. 8 are plotted the decay times of the 60/40/ $L_w$  series where the WW width  $L_w$  is changed from 120 to 190 Å (this series is doped: the 60/40/120 sample is not the same in Figs. 7 and 8, which explains the difference by a factor of 2). We observe a clear resonance effect around 140 Å but the decay time levels off at about 2 ps. These results do not exactly correspond to Fig. 4 of Ref.

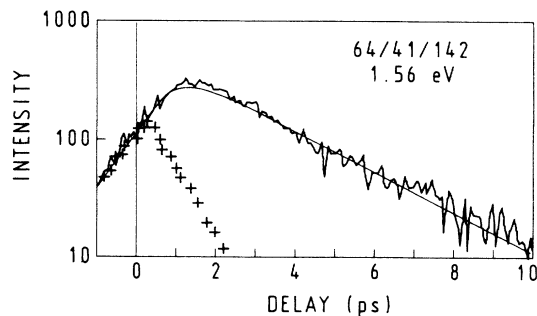


FIG. 6. Time-decay behavior of the 1.57-eV luminescence line in the 64/42/142 CQW. The solid line is a model fit to the time decay used to estimate the observed lifetime (see text). Intensity is in  $\log_{10}$  scale. In order to show the time resolution of the system, the time decay at 1.56 eV of an oxygen implanted GaAs sample (+) is also shown.

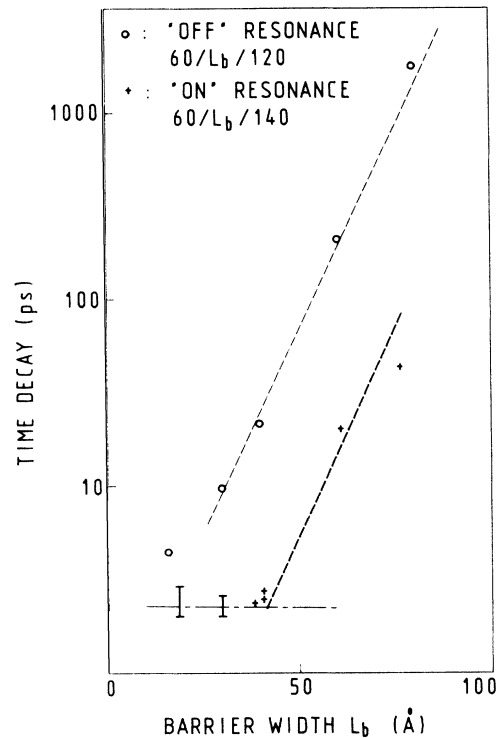


FIG. 7. Decay time of the first excited state luminescence in 60/ $L_b$ /140 samples as a function of the barrier width  $L_b$  (on resonance: +). Note the exponential decay down to about 40 Å and then the saturation at about 2 ps. The NW decay times are also reported for 60/ $L_b$ /120 samples (off resonance: ○). Times are in  $\log_{10}$  scale.

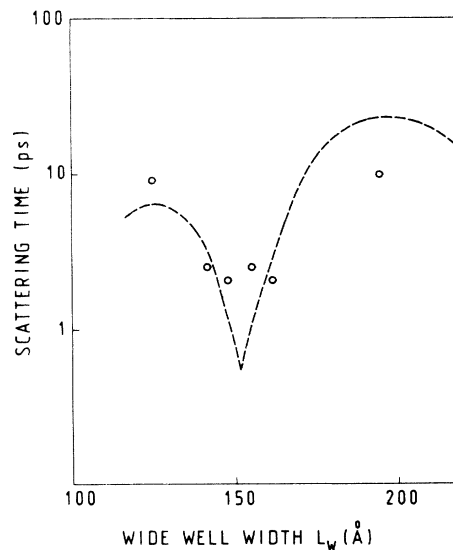


FIG. 8. Decay times of the NW luminescence in 60/40/ $L_w$  samples as a function of the wide well width  $L_w$ . The dashed curve represents the theoretical decay time when LO phonons are the main scattering mechanisms. Times are in  $\log_{10}$  scale.

25, as the barrier thickness of the two “off-resonance” samples have been measured to be 48 instead of 40 Å. The samples corresponding to the results plotted here have been grown with barrier thickness much closer to the expected value.

The difference by a factor of 2 between doped and undoped samples indicates a contribution of impurity scattering of the order of 20 ps, as observed for “on-resonance” samples when LO-phonon emission is not possible (see Sec. IV B).

One could wonder if the saturation observed in Figs. 7 and 8 around 2 ps is not in fact indicative of the limited time resolution of our system. In order to rule out this possibility, we show on Fig. 6 (together with the decay of sample 64/41/142) the decay time of an oxygen implanted GaAs sample at an energy (1.56 eV) close to the energy of the NW luminescence. This curve has a full width at half maximum (FWHM) of 930 fs and a decay time constant at 730 fs. This shows that the 2.2 ps decay time that we observe in the fastest samples is not limited by the system resolution.

Modeling of the time behavior, taking into account the pulse width (both the excitation and the up-conversion pulse) and the cooling of the electrons is plotted on Fig. 6 as a solid line (decay time: 2.2 ps; thermalization time: 0.3 ps; pulse width: 0.5 ps). The shape of the time decay curve at negative delays is due to the finite pulse width and is reproduced by a Lorentzian shape of 500-fs FWHM. We have as yet no good explanation for the very short thermalization time given by our crude model. This short value might be linked to the fact that the carriers are still hot when tunneling out.

### C. High-density effects

As already observed by Sauer *et al.*<sup>39</sup> and Alexander *et al.* in the case of  $\text{In}_{1-x}\text{Ga}_x\text{As}$  CQW's,<sup>40</sup> and in contrast with their results on  $\text{Al}_{1-x}\text{Ga}_x\text{As}$  CQW's,<sup>16</sup> the use of high-power excitation in our experiments leads to obvious saturation effects of the decay time. These effects can have two possible origins: a slowing down of the tunneling process due to electrostatic effects (spatial separation of electrons and holes due to the slower tunneling of holes<sup>10,16</sup>) or simply a Fermi filling of the levels of the large well preventing carriers to flow into the well. We shall evidence both processes in their respective density range.

Variation of the decay time constant with density is reported in Fig. 9, for the case of the 64/14/142 CQW (a qualitatively similar behavior is observed for all samples). This figure evidences a clear saturation of the transfer as the density is increased. Better understanding of the involved effects can be obtained by looking at Fig. 10, where the spectra of the same sample at different densities are reported, recorded 10 ps after the excitation pulse.

In the highest-density regime, the time decays clearly show two regimes: first a slow regime with time constant in excess of 100 ps, then a faster regime with time constant of the order of 40 ps. The slowest regime clearly corresponds to the case where the large well is filled. It

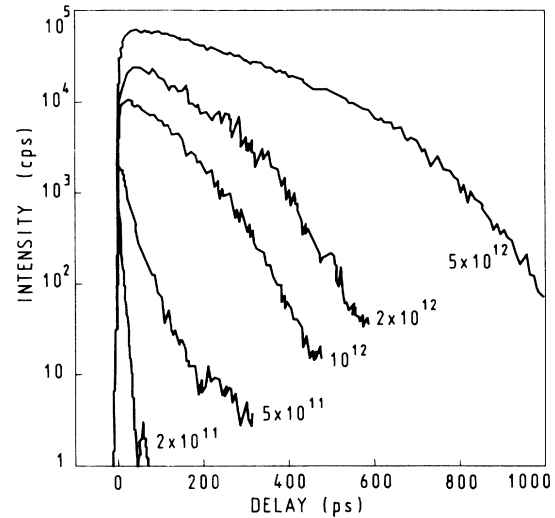


FIG. 9. High-density saturation effect on the time dependence of the luminescence intensity at 1.57 eV in the 64/42/142 sample. Corresponding injected carrier densities are indicated in the figure. Intensity is in  $\log_{10}$  scale.

indeed occurs as soon as the density is raised above  $10^{12} \text{ cm}^{-2}$  per well, i.e., when Fermi filling prevents electrons from being scattered out of the coupled levels.

These band filling effects are inferred from the spectrum of Fig. 10 with a density of  $2 \times 10^{12} \text{ cm}^{-2}$ : the luminescence intensity does not diminish above the 1.51-eV peak, but rather stays constant up to the 1.57-eV luminescence. This evidences that Fermi filling occurs, at least up to  $n = 2$ , for both the electron and the hole levels. Such a situation obviously prevents both carriers to relax down from the excited states to the ground state, they have to wait for sufficient radiative recombination before being able to relax down. Conservation of  $k$ -selection rules should give rise in such a case, to a constant

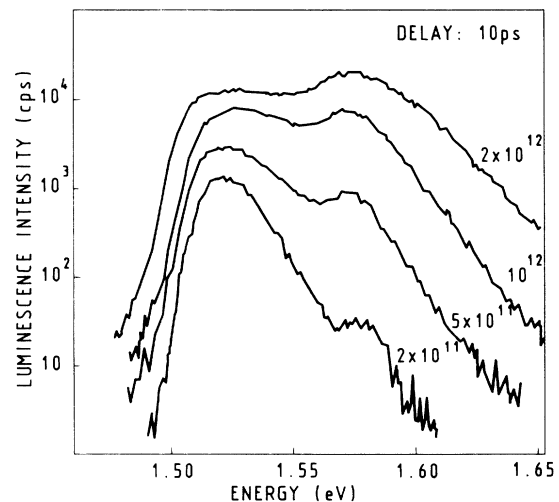


FIG. 10. High-density spectra, at a delay of 10 ps, for the 64/42/142 CQW. The different photocreated densities are indicated. Intensity is in  $\log_{10}$  scale.

luminescence intensity as a function of time. The decay observed here corresponds to the fact that the excitation of the sample is not homogeneous so that the different CQW's do not empty simultaneously. The break in the time decay curve at long time delays for the highest densities correspond to the density where band-filling effects no longer prevent the transfer of the carriers (densities below  $5 \times 10^{11} \text{ cm}^{-2}$ , see the corresponding spectra on Fig. 10). Basically, this break occurs when the Fermi-level position corresponds to the detection energy. A similar break is observed in highly excited single-quantum wells at the delay where the hole plasma changes from degenerate to nondegenerate.<sup>41</sup>

At densities below  $5 \times 10^{11} \text{ cm}^{-2}$ , another mechanism slows down the transfer: the faster tunneling of electrons (compared to holes) induces an electric dipole at the barrier thus causing misalignment of the electron levels. The decay rate is then given by a balance between the hole transfer rate from the NW to the WW and the "off-resonance" tunneling of the electrons. For a barrier of 40 Å, the decay of the NW luminescence is of the order of 40 ps both for resonant and nonresonant samples. It seems difficult to consider this time only as an electron tunneling: complete separation of the electrons and the holes at the high densities involved here would be impossible due to Fermi filling. The observed decay time of 40 ps might then be related to the transfer of holes and gives a very short time constant for heavy holes.

Different teams have considered this possible effect, both theoretically and experimentally.<sup>42-44</sup> Nido *et al.*<sup>43</sup> measured the hole tunneling time by inspection of the WW luminescence rise time. In our *p*-doped samples, such a procedure is not possible as the number of photoinjected holes is small compared to the background density. However, we have carried out the same study on the undoped samples with 40-Å barriers. At low densities, the decay time is about 20 ps, while the risetime of the WW luminescence is 40 ps (80-K measurements). When increasing the density, the decay time of the NW luminescence increases to about 40 ps and equals the rise time of the WW luminescence in the region where we expect dipole effects to dominate. This does confirm the importance of dipole effects at intermediate densities, and might imply a quite short tunneling time of holes. We shall try to estimate theoretically the involved times in Sec. IV C.

#### IV. INTERPRETATION

In order to interpret our results, we have carried out a set of calculations according to the method used by Ferreira and Bastard.<sup>23</sup> We compute the wave functions of the different levels in the CQW system and then estimate the times involved for the different scattering mechanisms by the Fermi golden rule. In order to compute the Fröhlich interaction we only take into account bulk phonon modes. In a first approximation, we shall not try to describe the electric field induced (in the dark or in high-density experiments) by the redistribution of holes from the narrow well to the large well. As a consequence, the well widths for which we compute resonance do not ex-

actly correspond to the actual widths of our samples, where the displacement of some of the holes from the NW to the WW is necessary to keep the Fermi level constant. This effect, however, was taken into account in the design of the samples: the difference between actual and computed widths is rather small and the main features of our experimental observations can be reproduced quite accurately. Our calculations use a band offset partition of 70–30%, the band gap of  $\text{Al}_{1-x}\text{Ga}_x\text{As}$ , the position of the spin-orbit split-off valence band and the heavy-hole effective mass are taken according to the following expressions:

$$E_g = 1.5192 + 1.36x_{\text{Al}} + 0.22x_{\text{Al}}^2,$$

$$\delta_{\text{s.o.}} = 0.341 - 0.066x_{\text{Al}},$$

$$m_{\text{hh}}^* = 0.38 + 0.31x_{\text{Al}},$$

where  $x_{\text{Al}}$  is the Al composition of the barrier. The Kane parameter is taken to be 24.2 eV and the longitudinal-phonon energy 36.7 meV.

#### A. Qualitative description

Let us first consider the case of exact resonance between the ground level of the NW and the second level of the WW. By exact resonance, we mean the case where these two levels are *exactly* at the same energy when the two wells are isolated from one another. We label  $|\phi_{1W}\rangle$  and  $|\phi_{2W}\rangle$  the wave functions of the first two levels in the isolated WW and  $|\phi_{1N}\rangle$  the wave function of the ground state of the isolated NW ( $E_{1W}$ ,  $E_{2W}$ , and  $E_{1N}$  their respective energies).

For barrier thickness large enough to neglect the overlap between  $|\phi_{1N}\rangle$  and  $|\phi_{1W}\rangle$ , the wave functions of the two coupled levels read

$$|\phi_{\pm}\rangle = (1/\sqrt{2})(|\phi_{1N}\rangle \pm |\phi_{2W}\rangle). \quad (1)$$

Therefore, in the limit of large barrier and exact resonance, the scattering time from  $|\phi_{+}\rangle$  or  $|\phi_{-}\rangle$  down to the ground state  $|\phi_{1W}\rangle$  of the CQW is exactly twice the scattering time from  $|\phi_{2W}\rangle$  to  $|\phi_{1W}\rangle$  in the isolated WW for the same scattering mechanism (LO-phonon scattering for example). In this case, the scattering time does not depend on the barrier thickness.<sup>25</sup>

This is indeed what we find if we adjust the WW thickness in our calculation in order to obtain its second level, when isolated, at exactly the same energy (64.754 61 meV) as the ground level of the isolated NW: this occurs for a WW thickness equal to 151.278 31 Å (this unphysical precision of 8 digits is necessary in order to obtain the calculated bonding and antibonding states extending over the two wells). Then we find (see Fig. 11), as expected from the simple treatment described above, that the relaxation (mediated by the LO-phonon emission through Fröhlich interaction) from the two coupled states does not depend on the barrier thickness and is close to 0.6 ps, twice the corresponding time in the isolated WW. The relaxation time remains the same for  $|\phi_{-}\rangle$  and  $|\phi_{+}\rangle$  as long as the energy splitting between the two states is small compared to one LO-phonon energy (36 meV).

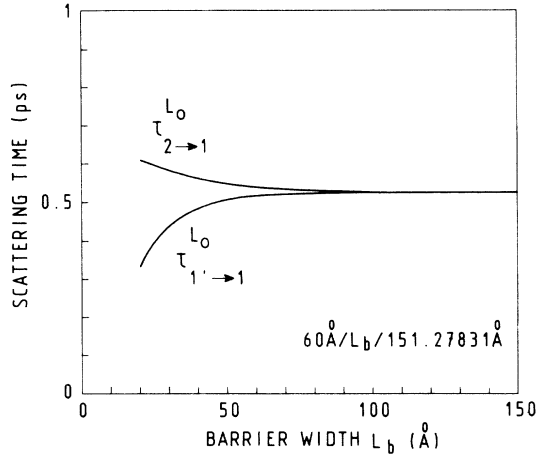


FIG. 11. LO-phonon scattering time of the coupled levels in the case of perfect resonance, as a function of the barrier thickness.

Deviation from this simple behavior is expected when the barrier thickness becomes very small, the overlap between  $|\phi_{1N}\rangle$  and  $|\phi_{1W}\rangle$  cannot be neglected anymore and the CQW system tends towards the single well, 211.278 31 Å wide: the two scattering times tend accordingly towards the interband scattering times from the second and third levels to the ground level. The main variation comes from the change of the emitted LO-phonon wave vector.

Let us now consider the case where we depart slightly from the exact resonance: a small variation in the thickness of one well, say the WW, results in a small mismatch  $\epsilon$  between  $E_{1N}$  and  $E_{2W}$  (uncoupled).  $|\phi_{1N}\rangle$  and  $|\phi_{2W}\rangle$  are no more in perfect resonance and  $|\phi_{\pm}\rangle$  are modified accordingly. If  $\delta$  is the level splitting in the case of exact resonance for the same barrier thickness, we may approximate, in the limit of large barriers, i.e., when  $\delta$  is much

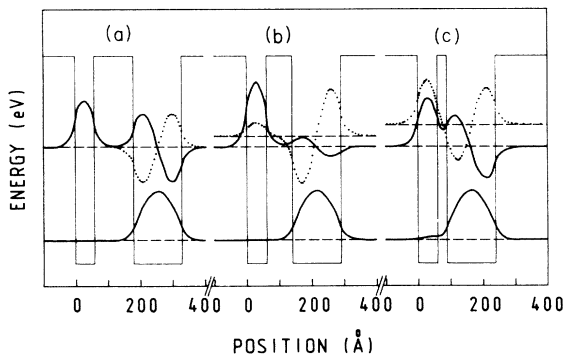


FIG. 12. Wave functions of the first three levels of a CQW system: (a) In the case of perfect resonance, 60/80/151.278 31. (b) In the case of a small mismatch and large barrier, 60/80/150. (c) In the case of small mismatch and narrow barrier, 60/30/150.

smaller than  $\epsilon$ , the two wave functions  $|\phi_{\pm}\rangle$  by

$$\begin{aligned} |\phi_{-}\rangle &= (1 - \delta/2\epsilon)|\phi_{1N}\rangle - (\delta/2\epsilon)|\phi_{2W}\rangle, \\ |\phi_{+}\rangle &= (\delta/2\epsilon)|\phi_{1N}\rangle + (1 - \delta/2\epsilon)|\phi_{2W}\rangle. \end{aligned} \quad (2)$$

The computed wave functions for the three cases of (a) exact resonance, (b) small detuning and large barrier, and (c) small detuning and narrow barrier are illustrated in Fig. 12. This figure shows that, for moderately large barriers, a very small detuning, corresponding to a very small variation in the WW thickness, localizes the wave function in one well or the other. The larger the barrier, the smaller the variation of the well thickness sufficient to destroy the resonance. On the contrary, for small barriers, a rather large mismatch can be overcome by the electronic coupling and the wave functions keep their extension over the two wells. In real samples, MBE grown, the uncertainty on the average thickness of each well is one or a few tenths of one angström. If the barrier is larger than 60 Å, this is sufficient to prevent the exact resonance and to localize  $|\phi_{-}\rangle$  in the NW and  $|\phi_{+}\rangle$  in the WW. If we consider the interface roughness assumed to be present in the best samples, i.e., of the order of one monolayer,<sup>45,46</sup> true resonance might only be obtained for barrier thickness narrower than 50 Å.

In Fig. 13(a), the calculated variations of the LO-phonon scattering time from  $|\phi_{-}\rangle$  down to  $|\phi_{1W}\rangle$  as a function of the barrier thickness, for different detunings (i.e., for different values of the WW thickness) are reported. The three curves corresponding to WW thickness of 151.278 31 Å (exact resonance), 151.2 Å and 151 Å indeed show that, in real samples, the exact resonance is practically impossible to achieve as soon as the barrier thickness is greater than 50 Å.

We have checked that in all cases the relaxation down to the ground state  $|\phi_{1W}\rangle$  is governed by the small proportion of the wave function  $|\phi_{-}\rangle$ , which is located in the WW [the second term of  $|\phi_{-}\rangle$  in (2)], even when this proportion is very small. This can be done by comparing the relaxation times obtained by calculating  $\langle \phi_{-} | H_{e-ph} | \phi_{1W} \rangle$  on the whole CQW structure or by taking into account only the parts of the wave function inside the WW,  $H_{e-ph}$  being the electron-phonon interaction. The two times obtained are nearly identical and this is due to the near complete localization of  $|\phi_{1W}\rangle$  in the WW. This is confirmed by Fig. 13(b), which shows the inverse of the probability density of state  $|\phi_{-}\rangle$  in the WW [the same values of barrier and well thickness were used in Figs. 13(a) and 13(b)]. We find that the variations of this parameter reproduce quite well the variations of the relaxation time: an exponential variation with a saturation for small barriers and an exponential domain that increases with the detuning.

Note that all the curves have nearly the same slope: it is easy to show within the transfer-matrix formalism that the exponential factor is equal to  $2KL_b$ , where  $K$  is the wave vector of  $|\phi_{-}\rangle$  inside the barrier [ $|\phi_{-}\rangle$  is taken to be equal to  $A \exp(Kz) + B \exp(-Kz)$  inside the barrier, in an envelope function model]. Since the energy of  $|\phi_{-}\rangle$  remains close to  $E_{1N}$ ,  $K$  is practically constant and depends only on the NW thickness. On the contrary, the

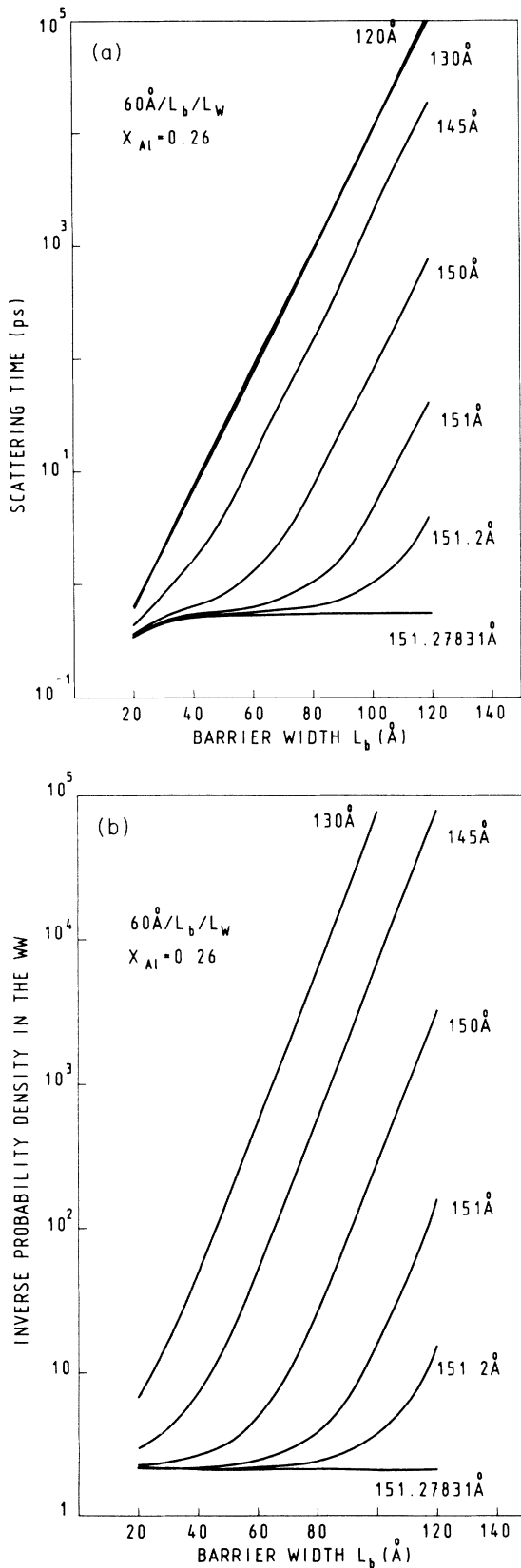


FIG. 13. (a) LO-phonon scattering time from  $|\Phi_{-}\rangle$  to  $|\phi_{1W}\rangle$  as a function of the barrier thickness, for different detunings. (b) Inverse of the density probability of  $|\Phi_{-}\rangle$  in the WW for the same parameters as in (a).

preexponential factor that gives the position of each curve and the value of barrier thickness above which the variation becomes exponential is strongly dependent on the detuning between the isolated NW and WW.

These results explain the exponential behavior observed in Fig. 7 even for “near-resonance” samples. The actual value of the barrier thickness above which the exponential variation begins to be observed (between 40 and 50 Å) would indeed correspond to a detuning of less than half one monolayer. The only basic difference between the samples designed to be “near” or “off” resonance is then the value of the energy mismatch between  $E_{1N}$  and  $E_{2W}$ .

In the same way, the above explanation may apply to the results obtained by Oberli *et al.*<sup>15</sup> and by Alexander *et al.*<sup>24</sup> on CQW’s tuned to resonance by applying an electric field: perfect resonance cannot be obtained, even for the case of a single set of CQW (Ref. 24), where inhomogeneous electric-field effects can be minimized. In fact, the resonance times observed by these two studies roughly fall on the exponential behavior observed on Fig. 7 for our “on-resonance” samples: 7.5 ps for a 50-Å barrier and 50 ps in the case of an 80-Å barrier. Both would correspond to a minimal detuning of the order of one monolayer.

The behavior evidenced in Fig. 8 is not well reproduced in our calculations. As a matter of fact, a sharp resonance down to 0.6 ps is expected to occur whatever the barrier thickness, see Fig. 14. This is quite different from the kind of leveling at 2 ps that we observe in our experiments. Let us recall here that the time resolution of the system is largely sufficient not to limit our measurements in this range. A crude analysis of the luminescence transient with a three level system (see the solid curve of Fig. 6) indicates that the decay time of 2.2 ps that we observe instead of the 0.6-ps time given by theory, cannot be explained by a slow cooling of the electrons. Such a slow cooling of the electrons would displace the time position of the maximum of the curve of Fig. 6, but would not affect in an appreciable manner its slope at long times. Note that the curves obtained under electric-field tuning both by Oberli *et al.*<sup>15</sup> and by Alexander *et al.*<sup>24</sup> also show a rather wide resonance around the minimum.

A possible explanation for the observed difference comes, once again, from the presence of imperfections existing in real samples. Interface roughness of typically one monolayer at each interface exists in the best samples,<sup>45,46</sup> and does not allow for the sharp resonance shown in Fig. 14. In order to take this kind of detuning into account, the simplest analysis would consist in averaging the times over a range of well-width values corresponding to the sample quality. Taking a variation of one monolayer at each interface would lead to averaging the curves of Fig. 14 over 5.8 Å on each side. This would smooth out the resonance dip with a characteristic time of about 1 ps in the case of 40-Å barriers, 2 ps for the case of 50-Å barriers, and 10 ps in the case of 80-Å barriers.

As a summary of this part, the actual classification of the samples can be the following.

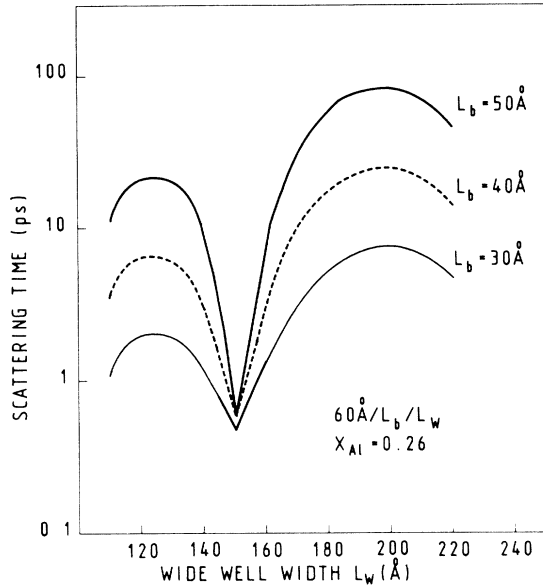


FIG. 14. LO-phonon-assisted scattering time from  $|\Phi_{-}\rangle$  to  $|\phi_{1W}\rangle$  as a function of the large well thickness, for different barrier thickness: 30, 40, and 50 Å. Times are in  $\log_{10}$  scale.

“Resonantly coupled” samples, where the two wave functions  $|\phi_{\pm}\rangle$  extend over the two wells with approximately the same probability. In this case the relaxation time from both of them to the ground state is equal to twice the intersubband relaxation time in the isolated WW. Note that the observed scattering time is much longer than the characteristic time corresponding to the energy splitting between the two coupled levels: the coherent picture is a good description.

“Decoupled” samples, where the energy mismatch cannot be overcome by the electronic coupling through the barrier and where the wave functions remain localized in one of the wells. The relaxation time from the NW down to the WW then varies as the inverse of the proportion of the NW wave function that extends in the WW.

### B. Quantitative comparison

If the experimentally observed tendencies are quite well reproduced by our calculations, both when the barrier thickness is changed and as a function of the WW width, we find a systematic difference by a factor of 2 to 3 between the observed and the calculated times. What we measure is the equivalent of intersubband scattering in isolated quantum wells, so we shall first recall the available results on this subject.

Intersubband scattering has long been the matter of a controversy; very different scattering times have been found.<sup>47–50</sup> Two main regimes are expected and indeed observed, depending on whether the separation between the involved levels is larger or smaller than the optical phonon energy.

Let us first consider the case of an energy separation larger than the optical-phonon energy. Very recently, an

intersubband scattering time of the order of 1 ps (this value might be slightly overestimated due to the participation of higher-lying states and to the experimental resolution) has been obtained in a rather indisputable way for a 158-Å quantum well.<sup>48</sup> The time of  $-2$  ps that we find here is in good agreement with this measurement as we do expect a difference by a factor of 2 between CQW’s and isolated wells.

When the energy separation is smaller than the optical-phonon energy, the scattering times are expected to be longer by orders of magnitude. Oberli *et al.*<sup>49</sup> indeed observed a scattering time of the order of 500 ps for a quantum well of 220 Å, and interpret this long time as corresponding to the emission of acoustical phonons. A much shorter value has, however, been reported recently.<sup>50</sup> For comparison, we have studied a 170/40/230 CQW; this sample being designed to be “on resonance,” but LO-phonon emission is not possible from  $|\phi_{\pm}\rangle$  down to  $|\phi_{1W}\rangle$ . We observe a decay time of about 40 ps (much longer than the 2-ps decay time observed on resonance when LO phonon is possible). This time is much shorter than the time observed by Oberli *et al.*,<sup>49</sup> but is in good agreement with the measurements of Levenson *et al.*<sup>50</sup> In any case, this measurement demonstrates the influence of LO-phonon emission in the decay from  $|\Phi_{\pm}\rangle$  to  $|\phi_{1W}\rangle$ . In the case of our samples, which are doped at a level of about  $10^{11}$  cm<sup>-2</sup> per well, the time of 40 ps might be explained by the large impurity concentration. Impurity scattering at this doping level would give rise to a resonance time of about 20 ps for a 40-Å barrier, in rather good agreement with our experimental observation.

Despite this rather good agreement between experimental results, we are left with a difference, by a factor of about 3 between the experimental values and the theoretical estimates. The difference might be due to screening effects, imperfections in the samples, high excitation density effects, possible influence of hole transfer between the wells, electric dipole effects, or high-carrier temperature influence.

We discard screening effects in a first approximation for two reasons.

(i) Leo *et al.*<sup>51</sup> have studied the thermalization of hot carriers due to interaction with the phonons in quantum wells of different doping levels, and at different excitation densities. Their conclusion is that background carriers are ineffective on changing the cooling rate, at least up to a doping level above  $10^{11}$  cm<sup>-2</sup> per well. This corresponds to the doping level of our samples.

(ii) Furthermore, we have compared one undoped 60/40/120 sample with a doped one. Contrary to what would be expected if screening occurs, we find a shorter decay time for the doped sample (9.5 instead of 20.5 ps).

Sample imperfections cannot be avoided, we have seen in the discussion that these imperfections might be responsible for the leveling off of the upper-state lifetime around resonance (see Fig. 8). However, we do not expect these imperfections to have an important effect far from resonance. As a matter of fact, the curves shown on Fig. 14 as a function of the WW width, will only be affected by sample imperfections close to the resonance, where the scattering times change abruptly with  $L_b$ . A

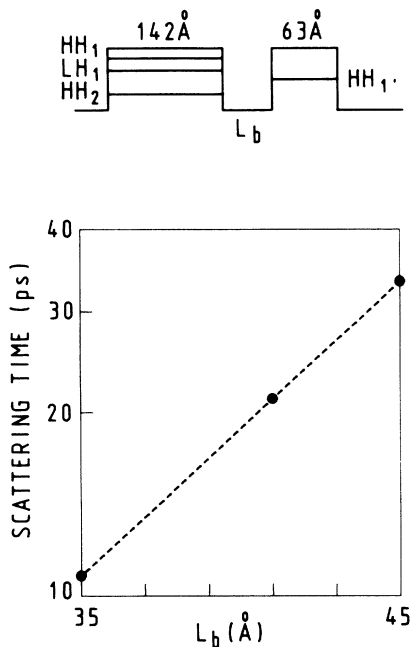


FIG. 15. Hole scattering time from a 60- to a 142-Å QW as a function of the barrier thickness. Times are in  $\log_{10}$  scale.

reduction of the transfer rate may be expected up to a time of about 1 ps, if we assume thickness fluctuations of the order of one monolayer at each interface.

High excitation density effects have been excluded in our discussion of the experimental results: we use an excitation density that is far below the doping level, and we have checked that our results are not sensitive to the excitation density in the domain where the experiments are performed. We shall come back to these effects in the next paragraph when discussing the experiments where the density was purposely raised.

Up to now, our calculations have been carried out without taking into account the possible transfer, in the dark, from part of the holes from the narrow well to the large well. This may affect the scattering times in a way that is very difficult to estimate as it is not strictly equivalent to applying a constant electric field to the whole system. We have not tried to estimate the transfer times when taking into account such effects.

Last, temperature effects (at short time the temperature of the electrons that are in the coupled levels is in excess of 200 K, see Fig. 4), may influence the scattering times. We have estimated the variation of the scattering rate with the energy of the carriers in each of the excited levels. Changing the energy of the electrons in the initial state indeed increases the scattering time. This change, however, is rather small as an increase of the energy by 100 meV only changes the scattering time from 0.6 to 1.3 ps. A mean energy of 17 meV (corresponding to a temperature of 200 K) would only increase the computed time up to 0.8 ps.

### C. Hole transfer and high-density effects

The decay time observed in the intermediate density regime (approximately  $10^{11}$   $\text{cm}^{-2}$  photoexcited carriers per well, see the curves of Fig. 10) might be explained by hole tunneling effects. Obviously this cannot simply be due to the tunneling of heavy holes. It has been shown by Ferreira and Bastard<sup>42</sup> that the strong mixing effects in the valence band could lead to increased transfer probabilities.

The impurity-assisted hole tunneling has been calculated for the case of the sample shown on Fig. 10 (142 Å/42 Å/63 Å), taking the heavy-hole ground-state  $\text{HH}'_1$  of the narrow QW as the initial state. To be consistent with the previous paragraphs, the band-bending effects have first been neglected. The impurities were assumed to sit on the two "inverted" GaAs/ $\text{Al}_{1-x}\text{Ga}_x\text{As}$  interfaces (areal concentration  $10^{10}$   $\text{cm}^{-2}$ ). Figure 15 shows the dependence of the hole tunneling time on the thickness of the barrier. We find that this time increases from 11 to 32 ps as the barrier thickness goes from 35 to 45 Å. These relatively short tunneling times are due to the small  $\text{LH}_1$ - $\text{HH}'_1$  splitting (2.2 meV) and are consistent with the experimental findings. Note that the reverse situation of hole transfer from a wide well to a narrow one<sup>44</sup> might give rise to longer times as a result of the smaller band-mixing effects in a narrow well.

### V. CONCLUSION

As a summary, in ideal CQW samples, *whatever the barrier thickness*, relaxation from the two resonant states  $|\Phi_{\pm}\rangle$  to the ground state  $|\phi_{1W}\rangle$  is expected to be limited by LO-phonon emission at 0.6 ps. In real samples different behaviors for the tunneling and the relaxation are evidenced.

"Resonantly coupled" samples, where the two wave functions  $|\phi_{\pm}\rangle$  extend over the two wells with approximately the same probability. We find experimentally a time of 2 ps for the relaxation to the ground state in that case, where the theory predicts 0.6 ps. The difference is partly explained by the imperfections in the sample and the high temperature of the carriers at short times.

"Decoupled" samples, where the energy mismatch cannot be overcome by the electronic coupling through the barrier and where the wave functions remain localized in one of the wells. The relaxation time from the NW down to the WW then varies as the inverse of the proportion of the NW wave function that extends in the WW. For a series of samples where the barrier thickness only is varied, we find an exponential behavior in agreement with theory.

### ACKNOWLEDGMENTS

The authors would like to thank M. Alexander, I. Bar Joseph, D. Hulin, B. Lambert, A. Levenson, W. W. Rühle, B. Sermage, and C. Tanguy for useful discussions and comments, P. Georges and F. Salin for their help in setting up the laser system, and Coherent Inc. for the loan of the double jet dye laser.

- <sup>1</sup>E. R. Brown, T. C. L. G. Sollner, C. D. Parker, W. D. Goodhue, and C. L. Chen, *Appl. Phys. Lett.* **55**, 1777 (1989).
- <sup>2</sup>J. F. Whitaker, G. A. Mourou, T. C. L. G. Sollner, and W. D. Goodhue, *Appl. Phys. Lett.* **53**, 385 (1988).
- <sup>3</sup>J. F. Young, B. M. Wood, G. C. Aers, R. L. S. Devine, H. C. Liu, D. Landheer, M. Buchanan, A. L. Springthorpe, and P. Mandeville, *Phys. Rev. Lett.* **60**, 2085 (1988).
- <sup>4</sup>L. Eaves, M. L. Leadbeater, D. G. Hayes, E. S. Alves, F. W. Sheard, G. A. Toombs, P. E. Simmonds, M. S. Skolnick, M. Henini, and O. H. Hughes, *Solid State Electron* **32**, 1101 (1989).
- <sup>5</sup>M. Tsuchiya, T. Matsutsue, and H. Sakaki, *Phys. Rev. Lett.* **59**, 2356 (1987).
- <sup>6</sup>E. T. Yu, M. K. Jackson, and J. C. McGill, *Appl. Phys. Lett.* **55**, 744 (1989).
- <sup>7</sup>S. Luryi, *Superlatt. Microstruct.* **5**, 375 (1989).
- <sup>8</sup>B. Deveaud, A. Chomette, A. Regreny, J. L. Oudar, D. Hulin, and A. Antonetti, in *High Speed Electronics*, edited by B. Källback and H. Beneking (Springer-Verlag, Berlin, 1986), p. 101.
- <sup>9</sup>Y. J. Chen, E. S. Koteles, B. S. Elman, and C. A. Armineto, *Phys. Rev. B* **36**, 4562 (1987).
- <sup>10</sup>R. Sauer, K. Thonke, and W. T. Tsang, *Phys. Rev. Lett.* **61**, 609 (1988).
- <sup>11</sup>Y. Tokuda, K. Kamamoto, N. Tsukuda, and T. Nakayama, *Appl. Phys. Lett.* **54**, 1232 (1989).
- <sup>12</sup>H. W. Liu, R. Ferreira, G. Bastard, C. Delalande, J. F. Palmier, and B. Etienne, *Appl. Phys. Lett.* **54**, 2082 (1989).
- <sup>13</sup>T. B. Norris, N. Vodjani, B. Vinter, C. Weisbuch, and G. A. Mourou, *Phys. Rev. B* **40**, 1392 (1989).
- <sup>14</sup>S. Luryi, *Solid State Commun.* **65**, 787 (1988).
- <sup>15</sup>D. Y. Oberli, J. Shah, T. C. Damen, T. Y. Chang, C. W. Tu, D. A. B. Miller, J. E. Henry, R. F. Kopf, N. Sauer, and A. E. DiGiovanni, *Phys. Rev. B* **40**, 3028 (1989).
- <sup>16</sup>M. G. W. Alexander, M. Nido, W. W. Rühle, R. Sauer, K. Ploog, K. Köhler, and W. T. Tsang, *Solid State Electron* **32**, 1621 (1989).
- <sup>17</sup>N. Sawaki, R. A. Höpfel, E. Gornik, and H. Kano, *Appl. Phys. Lett.* **55**, 1966 (1989).
- <sup>18</sup>A. Takeuchi, S. Muto, T. Inata, and T. Fujii, *Jpn. J. Appl. Phys.* **28**, 1741 (1989).
- <sup>19</sup>K. K. Cho, B. F. Levine, C. G. Bethea, J. Walker, and R. J. Malik, *Phys. Rev. B* **39**, 8029 (1989).
- <sup>20</sup>S. Ikeda, A. Shimizu, Y. Sekiguchi, M. Hasegawa, K. Kaneko, and T. Hara, *Appl. Phys. Lett.* **55**, 2057 (1989).
- <sup>21</sup>D. Ahn, *IEEE J. Quantum Electron.* **QE-25**, 2260 (1989).
- <sup>22</sup>T. Weil and B. Vinter, *J. Appl. Phys.* **60**, 3227 (1986).
- <sup>23</sup>R. Ferreira and G. Bastard, *Phys. Rev. B* **40**, 1074 (1989).
- <sup>24</sup>M. G. W. Alexander, M. Nido, W. W. Rühle, and K. Köhler, *Phys. Rev. B* **41**, 12 295 (1990).
- <sup>25</sup>B. Deveaud, F. Clérot, A. Chomette, A. Regreny, R. Ferreira, and G. Bastard, *Europhys. Lett.* **11**, 367 (1990).
- <sup>26</sup>In Ref. 25, we stated that the doping did not affect the transfer time. This mistake was due to a difference in the actual barrier thickness (40 and 48 Å) of the two samples used for the comparison.
- <sup>27</sup>In undoped quantum wells, the rise time of the luminescence at the band edge is of the order of 200 ps or more, and mainly related to the slow cooling of the carriers by acoustical phonons, see for example, J. I. Kusano, Y. Segawa, Y. Aoyagi, S. Namba, and H. Okamoto, *Phys. Rev. B* **40**, 1685 (1989).
- <sup>28</sup>T. Matsutsue and H. Sakaki, *Appl. Phys. Lett.* **50**, 1429 (1987).
- <sup>29</sup>J. Shah, T. C. Damen, B. Deveaud, and D. Block, *Appl. Phys. Lett.* **50**, 1307 (1987).
- <sup>30</sup>J. Shah, *IEEE J. Quantum Electron.* **QE-24**, 276 (1988).
- <sup>31</sup>The quantum-mechanical capture process in a quantum well is a very fast process: less than 1 ps [B. Deveaud, J. Shah, T. C. Damen, and W. T. Tsang, *Appl. Phys. Lett.* **52**, 1886 (1987)], the 200-ps rise time of the luminescence in quantum wells at low temperature is explained by the slow cooling of the photoexcited carriers down to lattice temperature.
- <sup>32</sup>P. Auvray, M. Baudet, A. Poudoulec, C. Guillemot, and A. Regreny, *J. Cryst. Growth* (to be published).
- <sup>33</sup>P. Auvray, M. Baudet, and A. Regreny, *J. Appl. Phys.* **62**, 456 (1987).
- <sup>34</sup>M. Baudet and P. Auvray (private communication).
- <sup>35</sup>G. Talalaeff, *Thin Solid Films* **150**, 369 (1987).
- <sup>36</sup>A. Pinczuck, J. Shah, R. C. Miller, A. C. Gossard, and W. Wiegmann, *Solid State Commun.* **50**, 735 (1984).
- <sup>37</sup>D. K. Ferry, M. A. Osman, R. Joshi, and M. J. Kann, *Solid State Electron* **31**, 401 (1988).
- <sup>38</sup>J. Feldman, G. Peter, E. O. Göbel, P. Dawson, K. Moore, C. Foxon, and R. J. Elliott, *Phys. Rev. Lett.* **59**, 2337 (1987).
- <sup>39</sup>R. Sauer, T. D. Harris, and W. T. Tsang, *Phys. Rev. B* **39**, 12 929 (1989).
- <sup>40</sup>M. W. Alexander, W. W. Rühle, R. Sauer, and W. T. Tsang, *Appl. Phys. Lett.* **55**, 885 (1989).
- <sup>41</sup>B. Deveaud, F. Clérot, A. Regreny, and K. Fujiwara (unpublished).
- <sup>42</sup>R. Ferreira and G. Bastard, *Europhys. Lett.* **10**, 279 (1989).
- <sup>43</sup>M. Nido, M. G. W. Alexander, W. W. Rühle, T. Schweizer, and K. Köhler, *Appl. Phys. Lett.* **56**, 355 (1990).
- <sup>44</sup>J. Shah, K. Leo, J. Gordon, T. C. Damen, D. A. B. Miller, J. E. Cunningham, and C. W. Tu, *Bull. Am. Phys. Soc.* **35**, 591 (1990).
- <sup>45</sup>C. Weisbuch, R. Dingle, A. C. Gossard, and W. Wiegman, *Solid State Commun.* **38**, 709 (1981).
- <sup>46</sup>B. Deveaud, J.-Y. Emery, A. Chomette, B. Lambert, and M. Baudet, *Appl. Phys. Lett.* **45**, 1078 (1984).
- <sup>47</sup>A. Seilmeyer, H. J. Hübner, G. Abstreiter, G. Weimann, and W. Schlapp, *Phys. Rev. Lett.* **59**, 1345 (1987).
- <sup>48</sup>M. C. Tatham, J. F. Ryan, and C. T. Foxon, *Phys. Rev. Lett.* **63**, 1637 (1989).
- <sup>49</sup>D. Y. Oberli, D. R. Wake, M. V. Klein, J. Klem, T. Henderson, and H. Morkoc, *Phys. Rev. Lett.* **59**, 696 (1987).
- <sup>50</sup>J. A. Levenson, G. Dolique, J. L. Oudar, and I. Abram, *Solid State Electron* **32**, 1869 (1989).
- <sup>51</sup>K. Leo, W. W. Rühle, and K. Ploog, *Phys. Rev. B* **38**, 1947 (1989).